ISSN 1063-7842, Technical Physics, 2009, Vol. 54, No. 4, pp. 561–568. © Pleiades Publishing, Ltd., 2009.
Original Russian Text © L.I. Goray, N.I. Chkhalo, G.E. Tsyrlin, 2009, published in Zhurnal Tekhnicheskoĭ Fiziki, 2009, Vol. 79, No. 4, pp. 117–124.

OPTICS, QUANTUM ELECTRONICS

Determining Angles of Incidence and Heights of Quantum Dot Faces by Analyzing X-ray Diffuse and Specular Scattering

L. I. Goray[a, b], N. I. Chkhalo[c], and G. E. Tsyrlin[a, d]

[a] *Institute of Analytical Instrument Making, Russian Academy of Sciences, Rizhskii pr. 26, St. Petersburg, 190103 Russia*
[b] *International Intellectual Group, Inc., 10313 Slated Island, New York, USA*
[c] *Institute for Physics of Microstructures, Russian Academy of Sciences, ul. Ul'yanova 46, Nizhni Novgorod, 603950 Russia*
[d] *St. Petersburg Physics and Technology Center for Research and Education, Russian Academy of Sciences, ul. Khlopina 8, St. Petersburg, 195220 Russia*
e-mail: lig@skylink.spb.ru

Received February 5, 2008

Abstract—Scattering of X rays by structures with multilayer ensembles of quantum dots MBE-grown in the In(Ga)As–GaAs system is studied by high-resolution grazing X-ray reflectometry. The peaks of the diffuse scattering intensity are discovered for the first time in structures with both vertically uncorrelated and vertically correlated quantum dots. It is shown that the position of the peak is totally determined by angle of inclination α of the quantum dot pyramidal faces (the so-called blaze condition for diffraction gratings), which was theoretically predicted earlier. Comparison with the results of scattering simulation carried out by the technique of boundary integral equations indicates that a simple geometrical condition allows one to exactly determine the value of α from the position of the intensity peak, the shape of which depends on many parameters. As follows from the theory and experiment, the width and height of the peaks for samples with vertically correlated quantum dots are larger than for those with uncorrelated dots. The roughness and interdiffusion of interfaces and the height of quantum dots are found from the position and amplitude of Bragg peaks. Thus, the conventional application of high-resolution grazing X-ray reflectometry is extended in this work to determination of the quantum dot geometry.

PACS numbers: 42.25.Dd, 42.25.Fx, 61.05.C-, 68.65.-k

DOI: 10.1134/S1063784209040185

INTRODUCTION

Low-temperature structures, such as quantum dots (QDs), quantum molecules, and quantum dot multilayer ensembles (QDMEs), are featured by certain linear sizes and angles of inclination of faces. The structural parameters of such self-organizing nanoobjects govern the electronic and optical performance of related devices and must be controlled easily and reliably. The geometry of nanostructures is related to the materials used and growth conditions and can be controlled in situ to an extent. However, the spread of the average values of geometrical parameters from experiment to experiment may be as high as several tens of percent even if experimental conditions are identical. Therefore, accurate online ex situ (preferably nondestructive) control of basic topological parameters of the structures is central for their characterization.

The methods of transmission electron microscopy (TEM) [1], atomic force microscopy (AFM) [2], and recently near-field scanning optical microscopy (NSOM) [3] have found wide application for analysis of nanodimensional objects; however, as regards detailed structural examination of QD-containing systems, these methods suffer from certain disadvantages. Specifically, the microscopic methods have considerable limitations in determining the averaged and compositional characteristics of nanoobject ensembles. For AFM, these limitations include a small scan area when high lateral and vertical resolutions are required, failure in "looking" into layers, and errors in measuring steep grades and acute angles. The problems inherent in TEM and NSOM are vertical calibration and gaining accurate quantitative characteristics of the QD geometry (including the heights and inclinations of faces) because of diffusion and the need to contrast the image. In addition, the TEM method is destructive and costly.

Application of X-ray radiation, especially its hard range and the short-wavelength part of the soft range, is a general-purpose nondestructive way of examining nanodimensional multilayer structures, specifically, the roughness of interfaces on the atomic scale and interdiffusion at interfaces. The methods of high-resolution X-ray diffractometry (HRXD) and reflectometry (HRXR), which study the distribution of the intensity of the X-ray scattering specular and diffuse components in the straight and reciprocal spaces, provide

much information for analysis of multilayer heterostructures, including those containing QDs.

HRXD and HRXR are well-developed techniques for analyzing the chemical composition, thickness, and crystal perfection of layers; elastic stress and dislocation distributions in the samples; and their fractality. The theory for such an analysis has been elaborated over the last few decades based both on the kinematic scattering approximation and on a general dynamic approach. Nevertheless, the potential of HRXD and HRXR is not used in full measure because of the difficulties associated with experimental data ambiguous interpretation and a large number of adjustable parameters appearing in models.

The advances in computer technology make it possible to apply rigorous numerical solution methods based on solving the Maxwell equations with exact boundary and radiation conditions. They do not require free parameters and are suitable for analysis of the optical scattering of short-wavelength electromagnetic radiation by a multilayer structure having large lateral period D, boundaries preset in an arbitrary form, and statistical inhomogeneities [4].

In this work, we investigate the specular and diffuse scattering of QDMEs in the In(Ga)As–GaAs system by high-resolution grazing X-ray reflectometry (HRGXR). Another goal is experimental detection of diffuse scattering peaks, the position of which depends on the inclination of the QD pyramidal faces (as was predicted theoretically in [5]).

1. EXPERIMENTAL

Using an EP-1203 setup for MBE, we grew three InAs–GaAs heteroepitaxial test structures (In(Ga)As layer on a single semi-insulating GaAs(100) substrate) with ten pairs of InAs–GaAs layers and a 5-nm-thick GaAs top layer: (i) with a wetting layer without QDs (F684), (ii) with vertically uncorrelated QDMEs (F680), and (iii) with completely correlated QDMEs (F681). The substrate temperature during growth was 483°C; the InAs deposition rate, 0.1 monolayer/s; and the GaAs deposition rate, 1 monolayer/s. The delay time before GaAs deposition (for structures F681 and F680) was 60 s. Thus, we deposited one monolayer (ML) of InAs (d_1 in thickness) for F684 and two MLs of InAs for F681 and F680. As a result, the thickness of the InAs wetting layer after QD formation became almost the same on all three structures, as confirmed by photoluminescence spectra. Thickness d_2 of GaAs spacers was about 9 nm for F684 and F681 and about 39 nm for F680. Under the given growth conditions, the QD density was $\approx 4 \times 10^{10}$ cm^{-2}; the QD height was $h \approx 5$ nm; and width L of the square base of the pyramid (the sides of which were oriented along the [110] and $[1\bar{1}0]$ crystallographic directions) was varied from ≈17 (lower layer) to ≈20 nm (upper layer) [6].

HRGXR measurements of the specular (coherent) and diffuse (partially coherent owing to the QD quasiperiodic distribution) scattering were taken using a Phillips ExpertPro reflectometer with a four-crystal Ge monochromator in the $\theta/2\theta$ scanning mode, detector scanning mode, and rocking curve mode at wavelength $\lambda_{\mathrm{Cu}K_{\alpha_1}} = 0.1541$ nm. The distance to the test structure was 320 mm; the slit width providing a sufficiently intense scattered signal, 100 μm (for slits 30 and 45 μm wide, the results were the comparable); the slit height, 1–5 mm; and the scanning pitch was selected from the interval 0.001°–0.005°, depending on desired resolution, at an angular divergence of the beam of 0.003°. The scattering in 3D structures that are uniform in two mutually perpendicular directions was measured with a position-sensitive slit detector. Such an approach is convenient for comparison with the reflectance calculated for 2D gratinglike structures. Integration of the differential scattering function over positions on the detector (or over spatial frequencies) somewhat smoothes the scattering curves. The same effect is reached by averaging calculated data for statistical sets of the structural parameters of the test structure.

To carry out optical computation in terms of a rigorous electromagnetic theory, we used the modified method of boundary integral equations [7], which proved to be exact and rapidly converging at large values of ratios D/λ and h/λ [8]. This is important, since large values of these ratios render any numerical approach difficult [9], especially as applied to structures with many randomized boundaries. Numerical experiments show [8] that the short-wavelength scattering intensity obtained for the statistical sets of the parameters of the structural model has a small dispersion, so that averaging over only several sets will suffice. The calculation error estimated from the energy balance is about 10^{-5} if 1000–1200 collocation points are used on each of the 21 boundaries of the structure being simulated and the method of convergence acceleration is applied [8]. When the scattering curve with a single statistical set of parameters was computed on a workstation having two Quad-Core Intel® Xeon® processors with a clock speed of 2.66 GHz, an 8-Mb L2 cache, a system bus with a clock speed of 1333 MHz, and a 16-Gb RAM, the computation time was about 45 min in the case of Windows Vista® Ultimate 64-bit operational system and eightfold parallelism.

2. STRUCTURAL MODEL

The physical model describing the QDME growth [10, 11] was used as the basis for a structural model of In(Ga)As–GaAs superlattices containing thin wetting InAs layers, which are separated by GaAs spacers, and pyramidal (triangular in the cross section) QDs with desired angles of inclination of faces. It is known [12, 13] that a perfect crystalline structure with vertically correlated QDMEs exhibits additional long-range order of

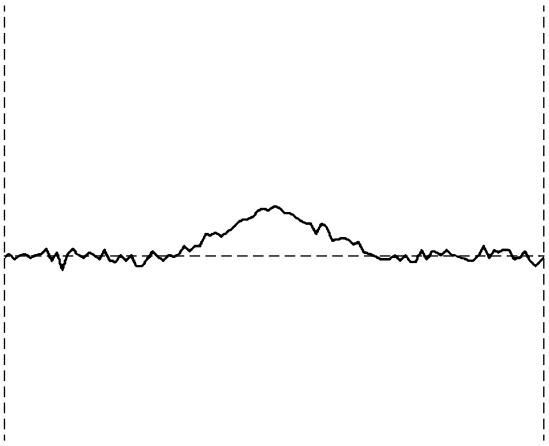

Fig. 1. Model of a boundary in the test structure (in section) containing a QD with a height of 4.9 nm, angle of inclination of 26.1°, random roughness with the rms deviation equal to 1.4 nm, and small correlation length.

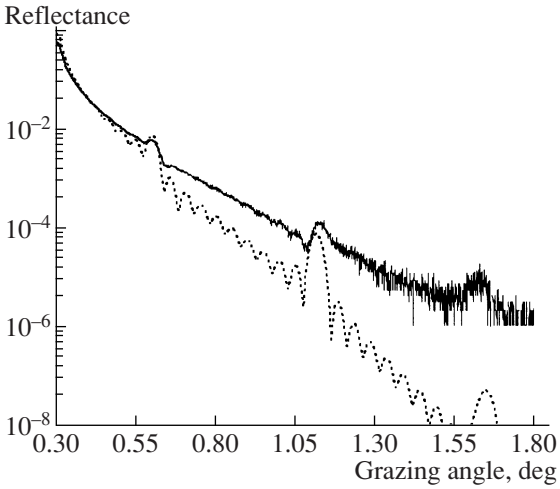

Fig. 2. Specular reflectance of structure F684 vs. radiation grazing angle relative to the growth plane along the [110] or $[1\bar{1}0]$ direction: solid line, measurement; dotted line, calculation.

QDs in the lateral (growth) plane, which results from the corrugation (undulation) of crystal planes and causes the quasi-periodic distribution of elastic strain and QDs [6].

In order to accurately take into account the QDME quasi-periodicity (the degrees of vertical and horizontal correlation of QDs) in diffraction computation, we used a model in which the grown structure with nonideal boundaries and QDs was represented as a multilayer superlattice with large period D that contains few or many random quasi-periodical irregularities. In this model, QDs lying in the lateral plane are ordered on average and the average distance between them depends on their density. For simplicity, we can assume that the random displacements of QDs from their average position do not correlate and that the displacement dispersion, QD size, and average distance between dots are the same in each layer. The degree of vertical correlation between QDs can be preset by randomly assigning a lateral displacement of one boundary relative to another. If QDMEs are highly correlated in the vertical direction, the rms deviation of such a displacement is small versus the QD width (that is, multiplication of QD ensembles takes place).

Given D, average distance between QDs, and QD average height and width (i.e., the inclination of faces), one can simulate variation of the horizontal and vertical correlations between QD structural parameters. In the model suggested, one can also set the surface corrugation of interfaces on which quasi-regular QDs are placed.

Randomly rough surfaces (with the Gaussian distribution of peak-to-peak heights and a Gaussian autocorrelation function) were generated using the spectral method [8] suitable for flat interface randomization. To set random roughness on QDs and corrugated boundaries, this method was extended for the case of interfaces prescribed by an arbitrary polygonal function (Fig. 1).

3. ANALYSIS OF SPECULAR SCATTERING

The specular reflection intensity normalized to the incident radiation intensity was measured with the aim to characterize the multilayer structures in general and find period $\Lambda = d_1 + d_2$, thickness ratio $\Gamma = d_1/\Lambda$, average error Δd of thickness measurements, and rms deviation σ of nanoroughness and interdiffusion.

The specular reflectance curve for structure F684 (Fig. 2) measured along one of the directions of interest exhibits three distinct Bragg peaks with ripple in between. This indicates that the crystal quality of the structure and, particularly, of the superlattice is high. Superlattice peaks are also clearly seen in the specular reflectance curve for structure F681 (reflection from the GaAs(004) plane, Fig. 3).

The measurements of the coherent reflection made on different structures with incident radiation aligned with one of the desired directions (the results are omitted here) suggest that the structures are fairly uniform. The parameters of the multilayer structures were determined from the positions and amplitudes of Bragg maxima and minima by the technique described in [14]. For F684, these parameters were found to be $\Lambda_{F684} =$ 8.20 nm (the as-grown value is ≈9.6 nm) and $\Gamma_{F684} =$ 0.073 (≈0.063). The amplitudes of the Bragg peaks suggest that the boundaries of the structures are essentially nonideal: the signs of nanoroughness and interdiffusion are present. The rms deviation of the roughness and interfacial diffusion determined for F684 by comparing the experimental and analytical specular reflectance curves (the latter were constructed using the Nevot–Croce model to take account of roughness) was

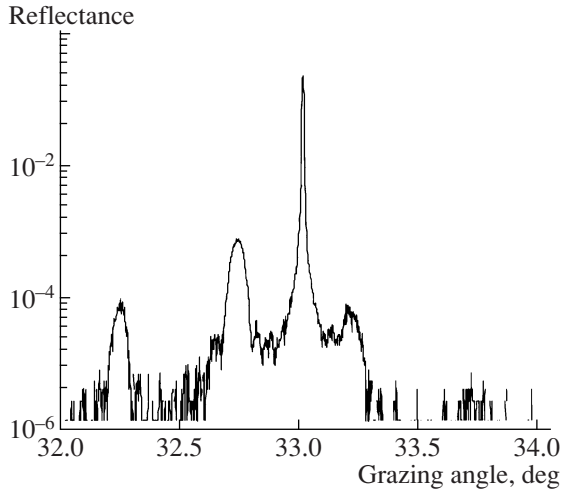

Fig. 3. Measured specular reflectance of structure F681 vs. radiation grazing angle relative to the growth plane along the [110] or [$1\bar{1}0$] direction (GaAs(004) reflection).

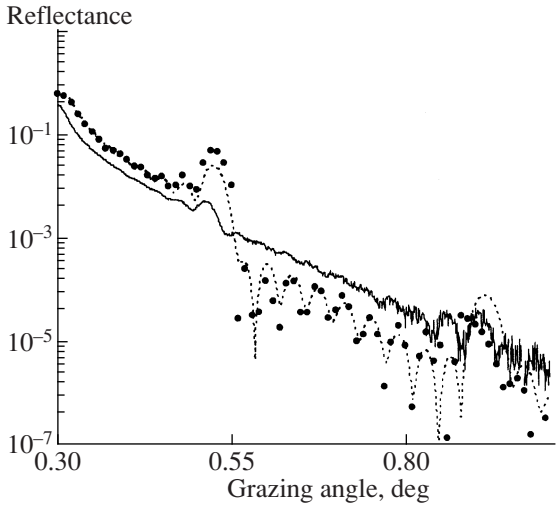

Fig. 4. Specular reflectance of structure F681 vs. radiation grazing angle relative to the growth plane along the [110] or [$1\bar{1}0$] direction: solid line, measurement; dotted line, approximate calculation; and filled circles, averaged rigorous calculation.

found to be $\sigma_{F684} = 1.4$ nm. The values of σ for different structures were determined with regard to thickness errors but without considering other nonuniformities, which may arise in the grown structures but analysis of which goes beyond the scope of this work.

The refractive indices of solids used to calculate σ were determined from the known atomic scattering factors [15] and apparently differ from the actual refractive indices of the grown layers, as indicated by low values of the reflectances measured at very small grazing angles. This is the main reason for the discrepancy between the measured and calculated reflectances, which is observed in Fig. 2.

Since the structures of superlattices F684 and F681 are close to each other, one, comparing their measured and calculated specular reflectances, can determine the influence of QDs in F681 on the decrease in the specular reflection intensity and on the average height of QDs. Such an approach is valid, since additional (QD-induced) component σ_{Q0} of the rms deviation of nanoroughness has an effect on the specular component that is comparable to the effect of other components responsible for the interface nonideality. For example, the reflectances measured for the two structures being compared differ by several tens of percent near the angle of total external reflection (Figs. 2, 4).

The average height of QDs was found from component σ_{Q0} with regard to their triangular (in the plane) shape [16], quasi-periodical arrangement over the layers, and fractality. Dispersion σ^2_{Q0} can be easily found from the effective rms deviation of roughness determined for F681 and dispersion linearity condition, $\sigma^2_{F681} = \sigma^2_{F684} + \sigma^2_{Q0}$. The QD height thus determined was $h_{aver} = 4.92$ nm, and the parameters of the multilayer structure obtained from comparison of the measured and calculated data were $\Lambda_{F681} = 10.37$, $\Gamma_{F681} = 0.116$, and $\Delta d_{F681} = 0.39$ nm. These values meet prescribed technological parameters. The influence of both quasi-regular QDs and random roughness of the boundaries on the scattering intensity can be described more accurately (compared with the use of conventional Nevot–Croce and Debye–Waller amplitude corrections) in terms of a rigorous computational model including plausible profiles of interfaces. The use of the above corrections may lead to a significant disagreement with the results of exact simulation, although numerical simulation may be difficult and require statistical averaging [8].

As follows from Fig. 4, the results obtained in terms of the rigorous model that are statistically averaged over as few as three sets of parameters yield specular reflection intensities that, in general, fit the measured data better than the approximate results (although some points require averaging over a larger number of statistical sets). This is true for grazing angles exceeding the angle of total external reflection, e.g., near the second Bragg peak, where an inaccuracy in the refractive indices used in calculation is less significant, so that the amount and type of roughness, including the QD shape, are the main factors influencing the reflectance.

4. ANALYSIS OF DIFFUSE SCATTERING

If structures have not only randomly rough boundaries but also quasi-periodically arranged QDs, the respective components in the diffuse scattering spectrum will be partially coherent. In general, the angular positions of these components are related to spatial frequencies and the amplitudes thereof are related to the

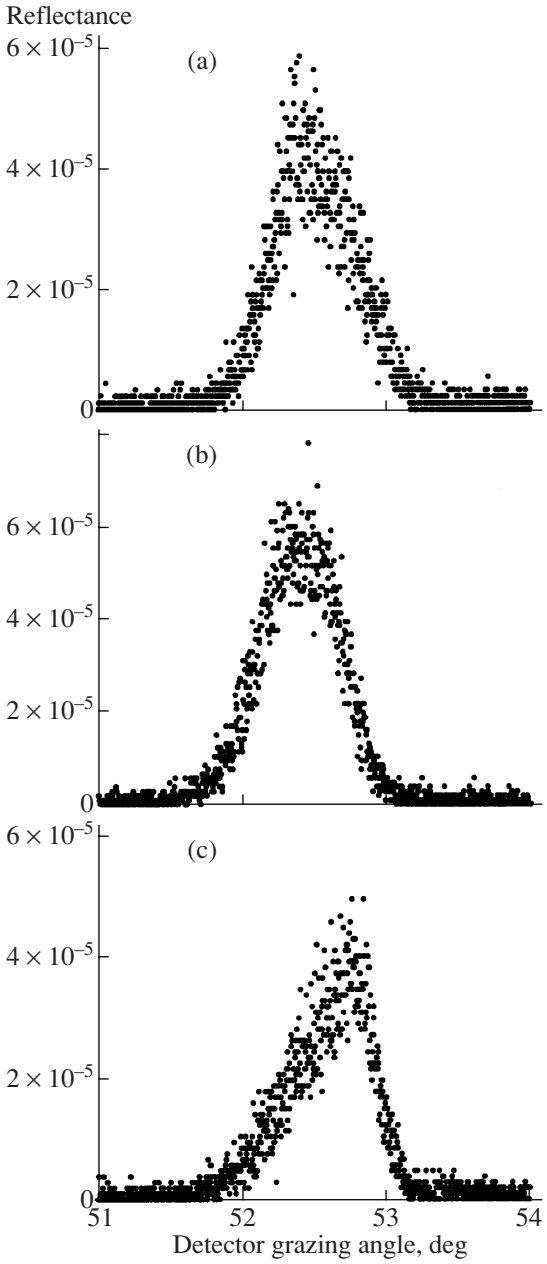

Fig. 5. Diffuse reflectance of structure F681 vs. detector grazing angle for radiation grazing angles of (a) 0.537°, (b) 0.570°, and (c) 0.620° relative to the growth plane along the [110] or [$1\bar{1}0$] direction.

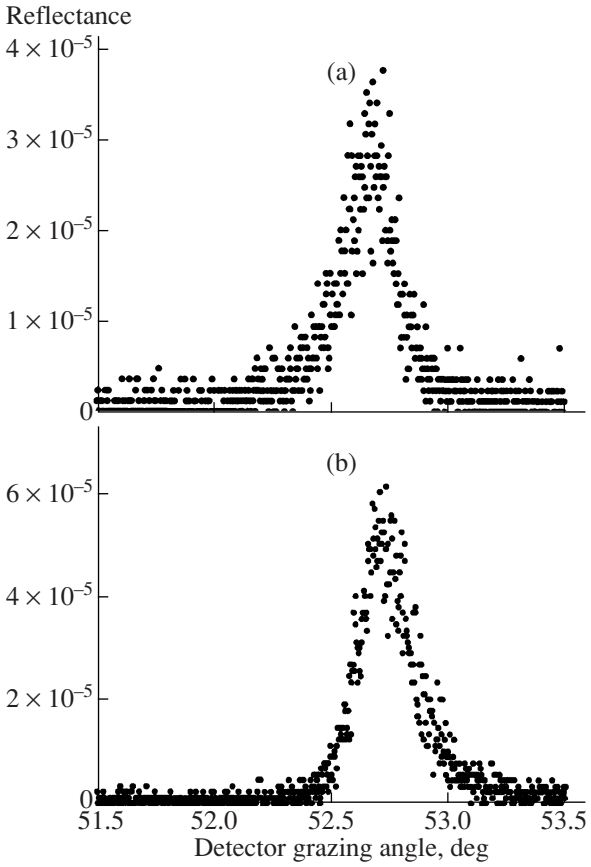

Fig. 6. Diffuse reflectance of structure F680 vs. detector grazing angle for radiation grazing angles of (a) 0.57° and (b) 0.75° relative to the growth plane along the [110] or [$1\bar{1}0$] direction.

Fourier coefficients in the expansions of the boundary profiles (i.e., to the boundary shapes) [17]. For layers with quasi-periodically arranged pyramidal QDs the bases of which are aligned with the [110] and [$1\bar{1}0$] directions and the faces of which are inclined at a certain angle, the scattering component with an angular position independent of the QD periodicity in the vertical and horizontal directions, QD height, and superlattice parameters and dependent on only the inclination of the faces is expected to grow. This is the so-called blaze condition for gratings, under which the reflected wave is amplified in the direction of specular reflection of the incident wave from the QD face [18].

To detect the peaks of diffuse scattering from QDMEs in structures F681 and F680 that result from amplification of waves reflected by the QD faces, incident radiation was aligned with either of the directions [110] and [$1\bar{1}0$] and the detector was scanned about grazing angle ζ_{dif}, which is given by

$$2\alpha = \zeta_{dif} - \zeta_{inc}, \quad (1)$$

where ζ_{inc} is the grazing angle of incident radiation and α is the angle of inclination of the QD faces ($\tan\alpha = 2h/L$).

Comparison with the results of simulation based on the rigorous electromagnetic theory [8] showed that simple geometrical relationship (1) accurately determines the positions of diffuse scattering intensity maxima at a given mean angle of inclination of the QD faces. The width and amplitude of these maxima can depend on various factors: spread of α, QD face nonideality, degree of correlation between QDs in the ver-

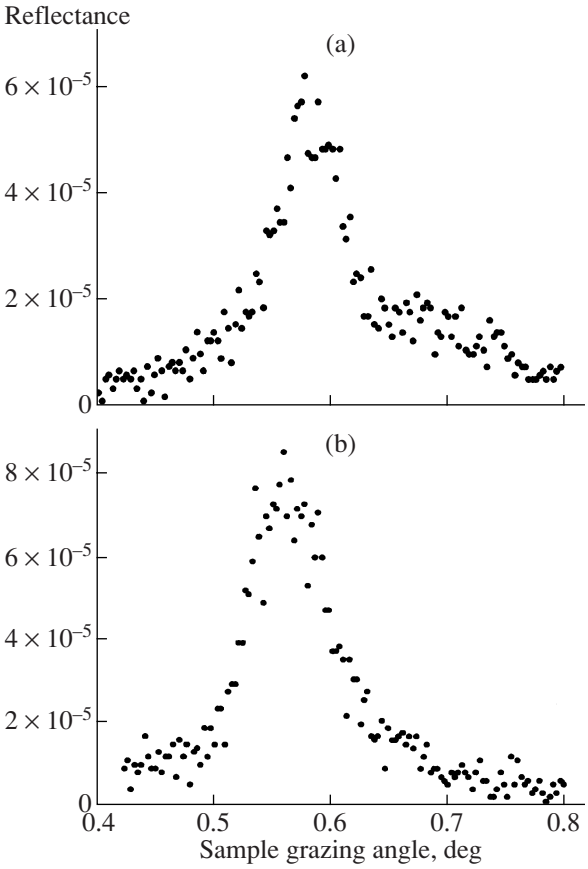

Fig. 7. Diffuse reflectance of structure F684 measured at a detector grazing angle of 52.8° vs. the test structure rocking angle relative to the growth plane along the (a) [110] or $[1\bar{1}0]$ and (b) $[1\bar{1}0]$ or [110] directions.

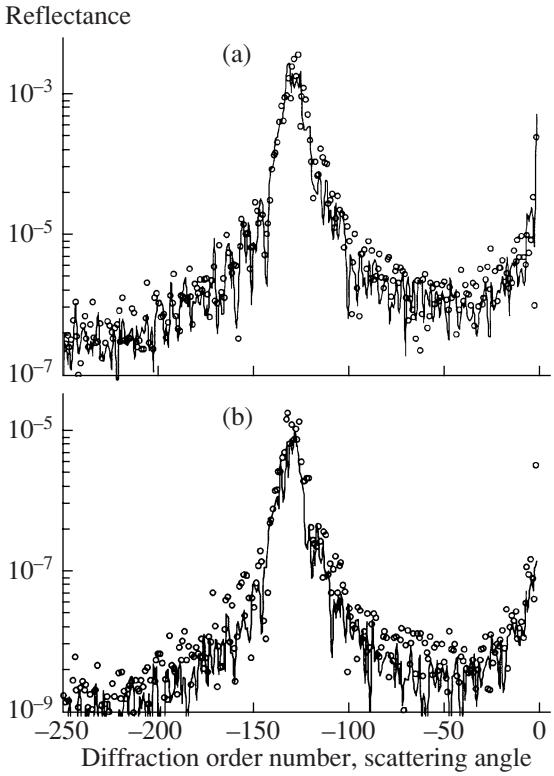

Fig. 8. Statistical averaged diffuse reflectance of structures F680 (solid lines) and F681 (circles) calculated vs. the scattering angle for different incident radiation grazing angles relative to the plane of incidence. Diffraction order no. –250 corresponds to a scattering grazing angle of ≈76.74°, the zeroth order corresponds to (a) –0.57° and (b) 1.00°, the intensity maximum near order no. –128 corresponds to a grazing angle of ≈52.75° (a), and the maximum near order no. –130 corresponds to ≈53.2° (b).

tical and horizontal directions, presence of long-range order in the QD arrangement in the growth plane, ζ_{inc}, and QD density, etc.

The mean values of inclination of the QD faces for structures F681 and F680 determined from the measured curves of diffuse scattering intensity turned out to be almost the same (Figs. 5, 6): $\alpha_{F681} \approx \alpha_{F680} = \alpha = 26.1°$ accurate to 0.1°. This value is close to a crystallographic angle of 26.6° the [311] direction makes with the growth direction. The mean width of QDs, which depends on the inclination and height of their faces, is $L = 20.1$ nm. This corresponds to the as-grown value for upper layers. As the grazing angle increases, the intensity peaks shift toward larger angles of scattering in accordance with expression (1).

The positions and angular dependence of the peaks thus determined are confirmed by rocking curves taken from structure F681 oriented along the [110] and $[1\bar{1}0]$ directions at a grazing angle of the detector of 52.8° (Fig. 7). From the data presented in the figures and from other measurements, it follows that the width and height of the intensity peaks for F681 exceed those for F680. This is explained by correlation between QDs in the vertical direction and supported by numerical computation.

Figure 8 shows the theoretical curves of diffuse scattering at incident radiation grazing angles $\zeta_{inc} = 0.57°$ (Fig. 8a) and $\zeta_{inc} = 1.0°$ (Fig. 8b). The curves were obtained for structures F681 and F680 using the mean parameters of the superlattices found in this work and statistical average sets of QD positions and heights including the boundary random roughness. The average angle of inclination of the QD faces determined by (1) from the position of the maximum in the diffuse scattering curves (the maximum near diffraction order of scattering no. –128 in Fig. 8a corresponds to a grazing angle of 52.75°; the maximum near diffraction order no. –130 in Fig. 8b, to an angle of –53.2°), as well as from the experimental curves for both angles and test structures, is almost the same and coincides, with a high accuracy, with the measured value ($\alpha_{calc} = \alpha = 26.1°$). The shift of the diffuse scattering peak with a change in the angle of incidence, which is predicted by exact calculations, is fairly accurately given by expression (1) (Fig. 8).

The calculated absolute amplitude of the diffuse scattering maxima and their width exceed the measured value roughly by an order of magnitude. For comparison to be correct, it is necessary to find a correction factor that reduces the 3D problem of scattering by pyramidal QDs to a 2D problem of scattering by a grating. The use of the correction factor requires that additional assumptions to be made. These are the QD uniform distribution in two mutually perpendicular planes of interest, proportionality between the scattering intensity and surface area of the scatterer (faces), and taking account of the shadow effect at a certain QD density. In addition, the degree of fractality and the presence of long-range order in the QD distribution should be preset. The correction factor in this work was not calculated, primarily because relevant data for the refractive indices of the materials used in the structures are lacking. Rough estimates show that such a comparison can generally be made and that the maximal experimental and theoretical values coincide in order of magnitude.

CONCLUSIONS

Using HRGXR, peaks of the diffuse scattering intensity were experimentally discovered for the first time in structures with vertically uncorrelated and correlated quantum dots. These peaks not only support the theoretical conclusions drawn earlier but also allow one to easily find the angles of inclination of the QD faces from the positions of the differential intensity maxima. Data on angles of inclination (QD widths) can be complemented by the values of QD heights obtained by comparing the measured and calculated reflectances of structures with and without QDs.

The method suggested in this work makes it possible to rapidly determine the orientation of the bases of QD faces. If incident radiation was not aligned with the [110] or $[1\bar{1}0]$ direction, which is perpendicular to QD faces, characteristic maxima of the diffuse scattering intensity were absent.

Thus, the conventional application of HRGXR determining the superlattice period, thickness of layers, and parameters characterizing the imperfection of layers and interfaces in heterostructures can be easily extended with this method for determining the angles of inclination of the faces and heights of self-organizing nanodimensional structures, such as QDs, quantum molecules, and QDMEs.

It was demonstrated that exact numerical computation using generated boundary profiles and appropriately chosen refractive indices of materials can basically yield the value of reflectance that is close to the experimental value even in the case of complex structures such as QDMEs. Rapid advances in table-top computing systems based on single-processor and multicore workstations, along with comprehensive investigation of quantum nanostructures and related materials, inspire hope that such a numerical analysis will be carried out in the near future.

In this and earlier works, we studied MBE-grown In(Ga)As–GaAs heterostructures. Note, however, that the above method of measuring and calculating structural parameters does not depend either on the technology of QD single- or multiple-layer ensembles or on materials used. Application of this method to structures in which QD faces have variable angles of inclination or are of a more complex configuration, e.g., have several slopes with different angles, is of interest. Such a situation can be encountered in heteroepitaxial Ge–Si structures with QDs [19].

ACKNOWLEDGMENTS

The authors thank Yu.A. Vainer, N.K. Polyakov, Yu.B. Samsonenko, and I.P. Soshnikov for assistance and valuable discussions.

This work was supported by the Russian Foundation for Basic Research (grant nos. 06-02-17331 and 05-02-17340) and the program "Low-Dimensional Quantum Structures" at the Presidium of the Russian Academy of Sciences.

REFERENCES

1. V. G. Talalaev, J. W. Tomm, A. S. Sokolov, I. V. Shtrom, B. V. Novikov, A. T. Winzer, R. Goldhahn, G. Gobsch, N. D. Zakharov, P. Werner, U. Gosele, G. E. Cirlin, A. A. Tonkikh, V. M. Ustinov, and G. G. Tarasov, J. Appl. Phys. **100**, 083704 (2006).
2. G. E. Tsyrlin, Yu. B. Samsonenko, V. N. Petrov, N. K. Polyakov, V. A. Egorov, S. A. Masalov, O. M. Gorbenko, A. O. Golubok, I. P. Soshnikov, and V. M. Ustinov, Pis'ma Zh. Tekh. Fiz. **26** (17), 59 (2000) [Tech. Phys. Lett. **26**, 781 (2000)].
3. A. Mintairov, Y. Chu, Y. He, J. Merz, V. Tokranov, S. Oktyabrsky, S. Blokhin, A. Kuzmenkov, E. Tanklevskaya, M. Maximov, and V. Ustinov, in *Proceedings of the 15th International Symposium on Nanostructures: Physics and Technology, Novosibirsk, 2007*, pp. 73–74.
4. L. I. Goray, Nucl. Instrum. Meth. A **536**, 211 (2005).
5. L. I. Goray, G. E. Cirlin, E. Alvers, Yu. B. Samsonenko, A. A. Tonkih, N. K. Polyakov, and V. A. Egorov, in *Proceedings of the 15th International Symposium on Nanostructures: Physics and Technology, Novosibirsk, 2007*, pp. 118–119.
6. G. E. Tsyrlin, V. N. Petrov, S. A. Masalov, and A. O. Golubok, Fiz. Tekh. Poluprovodn. (St. Petersburg) **33**, 733 (1999) [Semiconductors **33**, 677 (1999)].
7. L. I. Goray, J. F. Seely, and S. Yu. Sadov. J. Appl. Phys. **100**, 094901 (2006).
8. L. I. Goray, Proc. SPIE **6617**, 661 719 (2007).
9. A. Rathsfeld, G. Schmidt, and B. H. Kleemann, Commun. Comput. Phys. **1** (6), 984 (2006).
10. J. Tersoff, C. Teichert, and M. G. Lagally, Phys. Rev. Lett. **76**, 1675 (1996).
11. V. G. Dubrovski, G. E. Cirlin, Yu. G. Musikhin, Yu. B. Samsonenko, A. A. Tonkikh, N. K. Polyakov, V. A. Egorov,

A. F. Tsatsul'nikov, N. A. Krizhanovskaya, V. M. Ustinov, and P. Werner, J. Cryst. Growth **267**, 47 (2004).

12. N. N. Faleev, K. M. Pavlov, V. I. Punegov, A. Yu. Egorov, A. E. Zhukov, A. R. Kovsh, S. M. Mikhrin, V. M. Ustinov, M. Tabuchi, and Y. Takeda, Fiz. Tekh. Poluprovodn. (St. Petersburg) **33**, 1359 (1999) [Semiconductors **33**, 1229 (1999)].
13. V. A. Egorov and G. E. Tsyrlin, Pis'ma Zh. Tekh. Fiz. **26** (5), 86 (2000) [Tech. Phys. Lett. **26**, 220 (2000)].
14. E. Spiller, *Soft X-ray Optics* (SPIE, Bellingham, 1994).
15. http://www.cxro.lbl.gov/optical_constants.
16. J. C. Stover, *Optical Scattering: Measurement and Analysis* (SPIE, Bellingham, 1995).
17. V. A. Bushuev, Poverkhnost': Rentgenovskie, Sinkhrotronnye, Neitron. Issled., No. 9, 29 (2007).
18. M. C. Hutley, *Diffraction Gratings* (Academic, London, 1982).
19. O. P. Pchelyakov, Yu. B. Bolkhovityanov, A. V. Dvurechenskii, L. V. Sokolov, A. I. Nikiforov, A. I. Yakimov, and B. Foikhtlender, Fiz. Tekh. Poluprovodn. (St. Petersburg) **34**, 1281 (2000) [Semiconductors **34**, 1229 (2000)].